

Scalable Metric Learning via Weighted Approximate Rank Component Analysis

Cijo Jose François Fleuret
 Idiap Research Institute
 École Polytechnique Fédérale de Lausanne
 {firstname.lastname}@idiap.ch

Abstract

Our goal is to learn a Mahalanobis distance by minimizing a loss defined on the weighted sum of the precision at different ranks. Our core motivation is that minimizing a weighted rank loss is a natural criterion for many problems in computer vision such as person re-identification.

We propose a novel metric learning formulation called Weighted Approximate Rank Component Analysis (WARCA). We then derive a scalable stochastic gradient descent algorithm for the resulting learning problem. We also derive an efficient non-linear extension of WARCA by using the kernel trick. Kernel space embedding decouples the training and prediction costs from the data dimension and enables us to plug in arbitrary distance measures which are more natural for the features. We also address a more general problem of matrix rank degeneration & non-isolated minima in the low-rank matrix optimization by using new type of regularizer which approximately enforces the orthonormality of the learned matrix very efficiently.

We validate this new method on nine standard person re-identification datasets including two large scale Market-1501 and CUHK03 datasets and show that we improve upon the current state-of-the-art methods on all of them.

1. Introduction

Metric learning methods aim at learning a parametrized distance function from a labeled set of samples so that under the learned distance, samples with the same labels are nearby and samples with different labels are far apart [34]. Many fundamental questions in computer vision such as “How to compare two images? and for what information?” boil down to this problem. Among many such problems, person re-identification is the problem of recognizing individuals at different physical locations after they have been previously seen elsewhere. It is a challenging problem which recently received a lot of attention because of its importance in various application domains such as video surveillance, biometrics and behavior analysis [11].

The performance of person re-identification systems relies mainly on the image feature representation and the distance measure used to compare them. Hence the research in the field has focused either on designing features [7, 9, 42, 43] or on learning a distance function from a labeled set of images [23, 15, 18, 38].

It is difficult to analytically design features that are invariant to the various non-linear transformations that an image undergoes such as illumination, viewpoint, pose changes and occlusion. Furthermore even if such features were provided, the standard Euclidean metric would not be adequate as it does not take into account higher order dependencies on the feature representation. This motivates the use of metric learning for person re-identification.

Re-identification models are commonly evaluated by the cumulative match characteristic (CMC) curve. This measure indicates how the matching performance of the algorithm improves as the number of returned image increases. Given an algorithm and a test set of images of people with labels, each image in the test set is compared against the remaining images under the given algorithmic model and the position of the correct match is recorded. The CMC curve indicates for each rank the fraction of test samples which had that rank or better. A perfect CMC curve would reach the value 1 for rank #1.

In this paper we are interested in learning a Mahalanobis distance by minimizing a weighted rank loss such that the precision at the top rank positions of the CMC curve is maximized. We exploit ideas from Weston *et-al.* [35] to derive a metric learning algorithm which approximately minimizes a weighted rank loss efficiently using stochastic gradient descent. We then extend it to kernel space to handle distance measures which are more natural for the features we are dealing with. We also show that in kernel space SGD can be carried out more efficiently by using preconditioning [4, 23]. We also address a more general problem of matrix rank degeneration & non-isolated minima [20] in the low-rank matrix optimization by using new type of regularizer which approximately enforces the orthonormality of the learned matrix very efficiently. Our core contribution

is a generic and scalable algorithm to learn a Mahalanobis distance according to any weighted sum of the precisions at different ranks. This criterion in particular encompasses the AUC (i.e. uniform weighting) and the precisions at individual ranks (i.e. Dirac weighting).

We validate our approach on nine challenging person re-identification datasets: Market-1501 [44], CUHK03 [17], OpeReid [19], CUHK01 [16], VIPeR [12], CAVIAR [7], 3DPeS [2], iLIDS [45] and PRI450s [25], where we outperform other metric learning methods proposed in the literature.

2. Related works

Metric learning is a well studied research problem [40]. Most of the existing approaches have been developed in the context of the Mahalanobis distance learning paradigm [37, 34, 8, 13, 23, 15]. This consists in learning distances of the form

$$\mathcal{D}_M^2(x_i, x_j) = (x_i - x_j)^T M (x_i - x_j), \quad (1)$$

where M is a positive semi-definite matrix. Based on the way the problem is formulated the algorithms for learning such distances involve either optimization in the space of positive semi-definite (PSD) matrices, or learning the projection matrix W , in which case $M = W^T W$. Both of these approaches have advantages and disadvantages.

Optimization in the space of PSD matrices is a well understood convex optimization problem but the algorithms are computationally expensive [3]. Optimizing directly W is fast but the problem is no longer convex and hence gradient descent might get trapped in a local optima with poor performance. However in practice optimizing W does not result in poor generalization and this observation is supported by theoretical arguments [14]. We follow the approach of optimizing the projection matrix.

Large margin nearest neighbors [34] (LMNN) is a metric learning algorithm designed to maximize the performance of k -nearest neighbor classification in a large margin framework. Information theoretic metric learning [8] (ITML) exploits the relationship between the Mahalanobis distance and Gaussian distributions to learn a metric by minimizing the KL-divergence with a metric prior, like the identity matrix (Euclidean distance) while satisfying the data constraints such as the distance between the similar pairs should be less than a threshold and the distance between dissimilar pairs should be greater than a threshold. Many researchers have applied LMNN and ITML to re-identification problem with varying degree of success [25].

Pairwise Constrained Component Analysis (PCCA) [23] is a metric learning method that learns the low rank projection matrix W in the kernel space from sparse pairwise constraints. PCCA minimizes a generalized logistic loss, which pulls together similar pairs and pushes apart dissimi-

lar pairs. Xiong *et al.* [38] extended PCCA with a L^2 regularization term and showed that it further improves the performance.

Köstinger *et al.* [15] proposed the KISS (“Keep It Simple and Straight forward”) metric learning abbreviated as KISSME. Their method enjoys very fast training and they show good empirical performance and scaling properties compared to many other metric learning approaches. However the power of this method is limited by the fact that it can only capture up to the second order correlations present in the data.

Li *et al.* [18] consider learning a local thresholding rule for metric learning. They cast the problem into the support vector machine framework and it can be shown that they essentially learn the parameters of a binary linear SVM in a polynomial feature map defined on the pairs of points. However this method is computationally expensive to train, even with as few as 100 dimensions. Their paper discusses solving the problem in dual to decouple the dependency on the dimension but in practice it is solved in primal form with off-the-shelf solvers.

The performance of many kernel-based metric learning-based methods for person re-identification was evaluated in [38]. In particular the authors evaluated PCCA [23], variants of kernel Fisher discriminant (KFDA) analysis and reported that the KFDA variants consistently out-perform all other methods. The KFDA variants they investigated were Local Fisher Discriminant Analysis (LFDA) [28] and Marginal Fisher Discriminant Analysis (MFA) [39].

None of the above mentioned techniques explicitly models the objective that we are looking for in person re-identification, that is to optimize a weighted rank measure. We empirically compare our approach with rPCCA, LMNN, LFDA, KISSME, and SVMML, and we show that modeling this in the metric learning objective improves the performance.

There is an extensive body of work on optimizing ranking measures such as AUC, precision at k , F_1 score etc. Most of this work focuses on learning a linear decision boundary in the original input space, or in the feature space for ranking a list of items based on the chosen performance measure. A well known such model is the structural SVM [31]. In contrast here we are interested in ranking pairs of items by learning a metric. A related work is [22], where the authors study metric learning with different rank measures in the structural SVM framework. Wu *et al.* [36] used this framework to do person re-identification by optimizing the mean reciprocal rank criterion. Outside the direct scope of metric learning from a single feature representation, Paisitkriangkrai *et al.* [24] developed an ensemble algorithm to combine different base metrics in the structural SVM framework which leads to excellent performance for re-identification. Such an approach is complementary to

ours, as combining heterogeneous feature representations requires a separate additional level of normalization or the combination with a voting scheme.

Our work is inspired from WSABIE [35] and it is proposed for large-scale image annotation problem. Image annotation is a multi-label classification problem. WSABIE learns a multi-label classification model by simultaneously optimizing the precision in the top rank positions and a low dimensional joint embedding for both images and annotations. This work reports excellent empirical results in terms of accuracy, computational efficiency and memory footprint. Our work can be interpreted as a generalization of WSABIE for metric learning.

The work that is closely related to us is FRML [20] where they learn a metric similar to us by optimizing the WSABIE loss function. But their optimization scheme and the regularizer differ from us. Our approach is far more efficient computationally.

3. Weighted Approximate Rank Component Analysis

This section presents our metric learning algorithm, Weighted Approximate Rank Component Analysis (WARCA). Table 1 summarizes some important notations that we use in the paper.

Let us consider a training set of data point / label pairs:

$$(x_n, y_n) \in \mathbb{R}^D \times \{1, \dots, Q\}, n = 1, \dots, N. \quad (2)$$

Let \mathcal{S} be the set of indices of similar pairs of points from the training set defined as follows:

$$\mathcal{S} = \{(i, j) \in \{1, \dots, N\}^2, y_i = y_j\}. \quad (3)$$

For each label y we define the set \mathcal{T}_y of indices of samples of a class different from y :

$$\mathcal{T}_y = \{k \in \{1, \dots, N\}, y_k \neq y\}. \quad (4)$$

In particular, to each $(i, j) \in \mathcal{S}$ correspond a set \mathcal{T}_{y_i} .

Let W be a linear transformation that maps the data points from \mathbb{R}^D to $\mathbb{R}^{D'}$, with $D' \leq D$. For the ease of notation, we do not distinguish between matrices and their corresponding linear mappings. The distance function under the linear map W is given by:

$$\mathcal{F}_W(x_i, x_j) = \|W(x_i - x_j)\|_2. \quad (5)$$

Hereafter, x_i denote a the query point and we call other points as the ‘‘gallery set.’’ For a query point we define the rank of the a correct match x_j s.t $y_i = y_j$ from the gallery set as the number of incorrect matches whose distance is smaller than that of x_j , with respect to the distance function of Equation 5. This rank can be expressed as follows:

$$\mathcal{R}_W(i, j) = \sum_{k \in \mathcal{T}_{y_i}} \mathbb{1}_{\xi_{ijk} > 0}, \quad (6)$$

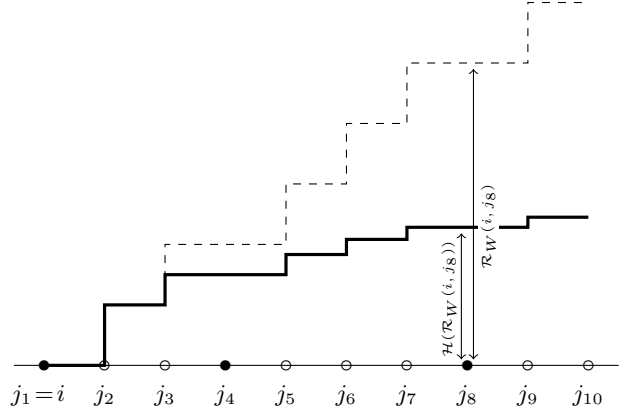


Figure 1: Given a query sample i , we define the rank of another sample j of the same class, with respect to that query, as a function of the number of samples of other classes closer to the query. The horizontal axis here corresponds to indexes of the samples sorted according to their similarities to the query sample. Black dots stand for samples of the same class as the query, and hollow circles for samples of different classes. The dashed line shows the uniform weighting of the rank, which increases by one unit each time we cross a sample of an incorrect class, and the thick line is the harmonic weighting, which increases in $1/n$. We used harmonic weighting for all our experiments.

Table 1: Notation

N	Number of training samples
D	Dimension of training samples
Q	Number of classes
$(x_i, y_i) \in \mathbb{R}^D \times \{1, \dots, Q\}$	i -th training sample
$\mathbb{1}_{\text{condition}}$	is equal to 1 if the condition is true, 0 otherwise
\mathcal{S}	the pairs of indices of samples of same class
\mathcal{T}_y	the indices of samples not of class y

where

$$\xi_{ijk} = \mathcal{F}_W(x_i, x_j) - \mathcal{F}_W(x_i, x_k). \quad (7)$$

See the dashed curve on Figure 1. Ideally we would like to learn the parameter W of the distance function of Equation 5 by minimizing the total rank of all queries from the training set and expect it to generalize well on the unseen samples. But minimizing directly the rank treats all the rank positions equally and usually in many problems including person re-identification we are interested in maximizing the correct match within the top few rank positions. This can be achieved by a weighting function $\mathcal{H}(\cdot)$ which penalizes more a drop in the rank at the top positions than at the bottom positions. In particular we use the rank weighting func-

tion proposed by Usunier *et al.* [32], which is of the form:

$$\mathcal{H}(M) = \sum_{m=1}^M \alpha_m, \alpha_1 \geq \alpha_2 \geq \dots \geq 0. \quad (8)$$

For example, using $\alpha_1 = \alpha_2 = \dots = \alpha_m$ (uniform weighting) will treat all rank positions equally, and using higher values of α s in top few rank positions will weight top rank positions more (e.g. harmonic weighting). Figure 1 illustrates uniform and harmonic weighting of the rank. So putting it all together, we would like to solve the following optimization problem:

$$\min_W \frac{1}{|\mathcal{S}|} \sum_{(i,j) \in \mathcal{S}} \mathcal{H}(\mathcal{R}_W(i,j)). \quad (9)$$

With the convention that $\frac{0}{0} = 0$, we rewrite Equation 9 as follows [35]:

$$\min_W \frac{1}{|\mathcal{S}|} \sum_{(i,j) \in \mathcal{S}} \sum_{k \in \mathcal{T}_{y_i}} \mathcal{H}(\mathcal{R}_W(i,j)) \frac{\mathbb{1}_{\xi_{ijk} > 0}}{\mathcal{R}_W(i,j)}. \quad (10)$$

3.1. Max-Margin Reformulation

The metric learning problem in equation 10 aims at minimizing the 0-1 loss, which is a difficult optimization problem. In order to make it tractable we upper-bound this loss with the hinge one [26] with margin γ . Also, to control the capacity of the model, we add an approximate orthonormal regularizer on the parameters we are estimating. This is equivalent to minimizing the following loss function:

$$\mathcal{L}(W) = \frac{\lambda}{2} \|WW^T - I\|^2 + \frac{1}{|\mathcal{S}|} \sum_{(i,j) \in \mathcal{S}} \sum_{k \in \mathcal{T}_{y_i}} \mathcal{H}(\mathcal{R}_W^\gamma(i,j)) \frac{|\gamma + \xi_{ijk}|_+}{\mathcal{R}_W^\gamma(i,j)}, \quad (11)$$

where I is the identity matrix and $\mathcal{R}_W^\gamma(i,j)$ is the margin penalized rank given as follows:

$$\mathcal{R}_W^\gamma(i,j) = \sum_{k \in \mathcal{T}_{y_i}} \mathbb{1}_{\gamma + \xi_{ijk} > 0}. \quad (12)$$

The intuition for approximate orthonormal regularizer comes from algorithms such PCA or FDA. These algorithms ensure that the learned linear transformation is orthonormal and it comes from the Gaussian assumptions on the data distribution by these algorithms. This strong prior assumption helps when the dataset is small or when it follows a Gaussian distribution. But it under-fits when the data is large and does not follow a Gaussian distribution. Therefore we relax this constraint in our algorithm to satisfy it approximately with a controlling parameter λ which can

be cross-validated. Moreover this readdresses the general problem of low-rank matrix optimization, that is directly optimizing the low-rank matrix W may result in W not invariant to orthonormal transformation ie $W^T W \neq I$ and result in non-isolated minimizers [20]. A cheap way to approximately get rid of this issue is to use our regularizer. We do not want the W matrix to be fully invariant to orthonormal transformation because it may not capture the data manifold correctly. Thus our regularizer acts as a perfect trade-off. We noticed empirically a faster convergence of SGD with our regularizer than with L2 regularizer and the above might be the reason.

The loss function in 11 is very similar to WSABIE [35]. Weston *et al.* [35] showed that WSABIE can be efficiently solved by using stochastic gradient descent and we follow the same approach. An unbiased estimator of the empirical loss can be obtained by following sampling procedure:

1. Sample (i,j) uniformly at random from \mathcal{S} .
2. For the selected (i,j) uniformly sample $k \in \mathcal{T}_{y_i} : \gamma + \xi_{ijk} > 0$, i.e. from the set of incorrect matches scored higher than the correct match x_j .

The sampled triplet (i,j,k) has a contribution of $\mathcal{H}(\mathcal{R}_W^\gamma(i,j))|\gamma + \xi_{ijk}|_+$ because the probability of drawing a k in step 2 from the violating set is $\frac{1}{\mathcal{R}_W^\gamma(i,j)}$ [35].

We use the above sampling procedure to solve WARCA efficiently using mini-batch stochastic gradient descent (SGD) with Nesterov's momentum [29], which is found to converge faster empirically compared to vanilla SGD. Algorithm 1 describes a vanilla SGD for WARCA, without the mini-batch and momentum.

Let Z denote the number of times the loop gets executed in the step 8-12 of the algorithm 1. It follows a geometric distribution:

$$P(Z = z) = (1 - p)^{z-1} p, \quad (13)$$

where

$$p = \frac{\mathcal{R}_W^\gamma(i,j)}{|\mathcal{T}_{y_i}|}. \quad (14)$$

Which leads to

$$E(Z) = \frac{1}{p} = \frac{|\mathcal{T}_{y_i}|}{\mathcal{R}_W^\gamma(i,j)}. \quad (15)$$

and motivates the use of the following approximation

$$\hat{\mathcal{R}}_W^\gamma(i,j) = \left\lfloor \frac{|\mathcal{T}_{y_i}|}{z} \right\rfloor, \quad (16)$$

which can be shown to be an upper bound of the true rank $\mathcal{R}_W^\gamma(i,j)$ by at most a factor $\frac{\ln p}{p-1} \geq 1$.

Algorithm 1 Stochastic gradient descent algorithm for WARCA

Input: Label vector $y \in \{1, \dots, Q\}^N$, Data matrix $X \in \mathbb{R}^{D \times N}$, Regularizer $\lambda \geq 0$, Initial solution $W_0 \in \mathbb{R}^{D' \times D}$, Step size η , Margin γ

- 1: $\mathcal{S} = \{(i, j) \in \{1, \dots, N\}^2, y_i = y_j\}$
- 2: $\forall y_i \in y, \mathcal{T}_{y_i} = \{k \in \{1, \dots, N\}, y_k \neq y_i\}$
- 3: $t = 0$
- 4: **while** (not converged) **do**
- 5: Sample (i, j) uniformly at random from \mathcal{S}
- 6: $d_{ij} = \mathcal{F}_W(x_i, x_j)$
- 7: $z = 0$
- 8: **do**
- 9: Sample k uniformly at random from \mathcal{T}_{y_i}
- 10: $d_{ik} = \mathcal{F}_W(x_i, x_k)$
- 11: $z = z + 1$
- 12: **while** $z \leq |\mathcal{T}_{y_i}|$ or $\gamma + d_{ij} > d_{ik}$
- 13: $W_{t+1} = W_t - 2\eta\lambda(W_t W_t^T - I)W_t$
- 14: **if** $\gamma + d_{ij} > d_{ik}$ **then**
- 15: $W_{t+1} = W_{t+1} - 2\eta\mathcal{H}\left(\left\lfloor \frac{|\mathcal{T}_{y_i}|}{z} \right\rfloor\right) \nabla_W |\gamma + \xi_{ijk}| +$
- 16: **end if**
- 17: $t = t + 1$
- 18: **end while**
- 19: Output W_t

3.2. Kernelization

Most commonly used features in person re-identification are histogram-based such as LBP, SIFT BOW, RGB histograms to name a few. The most natural distance measure for histogram-based features is the χ^2 distance [41]. Most of the standard metric learning methods work on the Euclidean distance with PCCA being a notable exception. To plug any arbitrary metric which is suitable for the features, such as χ^2 , one has to resort to explicit feature maps [33] that approximates the χ^2 metric. However, it blows up the dimension and the computational cost. Another way to deal with this problem is to do metric learning in the kernel space, which is the approach we follow.

Let W be spanned by the samples:

$$W = AX^T = A \begin{pmatrix} x_1^T \\ \dots \\ x_N^T \end{pmatrix}. \quad (17)$$

which leads to

$$\mathcal{F}_A(x_i, x_j) = \|AX^T(x_i - x_j)\|_2, \quad (18)$$

$$= \|A(\kappa_i - \kappa_j)\|_2. \quad (19)$$

Where κ_i is the i^{th} column of the kernel matrix $K = X^T X$.

Then the loss function in (11) becomes:

$$\mathcal{L}(A) = \frac{\lambda}{2} \|AKA^T - I\|^2 + \frac{1}{|\mathcal{S}|} \sum_{(i,j) \in \mathcal{S}} \sum_{k \in \mathcal{T}_{y_i}} \mathcal{H}(\mathcal{R}_A^\gamma(i, j)) \frac{|\gamma + \xi_{ijk}|_+}{\mathcal{R}_A^\gamma(i, j)}, \quad (20)$$

with

$$\xi_{ijk} = \mathcal{F}_A(x_i, x_j) - \mathcal{F}_A(x_i, x_k). \quad (21)$$

Apart from being able to do non-linear metric learning, kernelized WARCA can be solved efficiently again by using stochastic sub-gradient descent. If we use the inverse of the kernel matrix as the pre-conditioner of the stochastic sub-gradient, the computation of the update equation, as well the parameter update, can be carried out efficiently. Mignon *et. al* [23] used the same technique to solve their PCCA, and showed that it converges faster than vanilla gradient descent. We use the same technique to derive an efficient update rule for our kernelized WARCA. A stochastic sub-gradient of Equation 20 with the sampling procedure described in the previous section is given as:

$$\nabla L(A) = 2\lambda(AKA^T - I)AK + 2\mathcal{H}(\mathcal{R}_A^\gamma(i, j)) A \mathbb{1}_{\Upsilon_{ijk}(A) > 0} \mathcal{G}_{ijk}, \quad (22)$$

where

$$\Upsilon_{ijk}(A) = \gamma + \mathcal{F}_A(x_i, x_j) - \mathcal{F}_A(x_i, x_k), \quad (23)$$

and

$$\mathcal{G}_{ijk} = \frac{(\kappa_i - \kappa_j)(\kappa_i - \kappa_j)^T}{d_{ij}} - \frac{(\kappa_i - \kappa_k)(\kappa_i - \kappa_k)^T}{d_{ik}}, \quad (24)$$

where

$$d_{ij} = \mathcal{F}_A(x_i, x_j), \quad (25)$$

$$d_{ik} = \mathcal{F}_A(x_i, x_k). \quad (26)$$

Multiplying the right hand side of Equation (22) by K^{-1} :

$$\nabla \mathcal{L}(A)K^{-1} = 2\lambda(AKA^T - I)A + 2\mathcal{H}(\mathcal{R}_A^\gamma(i, j)) AK \mathbb{1}_{\Upsilon_{ijk}(A) > 0} \mathcal{E}_{ijk}. \quad (27)$$

with

$$\mathcal{E}_{ijk} = K^{-1} \mathcal{G}_{ijk} K^{-1} \quad (28)$$

$$= \frac{(e_i - e_j)(e_i - e_j)^T}{d_{ij}} - \frac{(e_i - e_k)(e_i - e_k)^T}{d_{ik}}. \quad (29)$$

where e_l is the l^{th} column of the canonical basis that is the vector whose l^{th} component is one and all others are

zero. In the preconditioned stochastic sub-gradient descent we use the updates of the form:

$$A_{t+1} = (I - 2\lambda\eta(A_t K A_t^T - I))A_t - 2\eta\mathcal{H}(\mathcal{R}_A^\gamma(i, j))A_t K \mathbb{1}_{\Upsilon_{ijk}(A_t) > 0} \mathcal{E}_{ijk}. \quad (30)$$

Please note that \mathcal{E}_{ijk} is a very sparse matrix with only nine non-zero entries. This makes the update extremely fast. Preconditioning also enjoys faster convergence rates since it exploits second order information through the preconditioning operator, here the inverse of the kernel matrix [4].

4. Experiments

We evaluate our proposed algorithm on nine standard person re-identification datasets. We first describe the datasets and baseline algorithms and then present our results.

4.1. Datasets and baselines

The largest dataset we experimented with is the **Market-1501** dataset [44] which is composed of 32,668 images of 1,501 persons captured from 6 different view points. It uses DPM [10] detected bounding boxes as annotations. **CUHK03** dataset [17] consists of 14,096 images of 1,467 persons and it has both DPM detected and manually annotated bounding boxes. **OpeReid** dataset [19] consists of 7,413 images of 200 persons. **CUHK01** dataset [16] is composed of 3,884 images of 971 persons, with two pairs of images per person, each pair taken from a different viewpoint. Each image is of resolution 160×60 . The most popular and challenging person re-identification dataset is the **VIPeR** [12] dataset. It consists of 1,264 images of 632 person, with 2 images per person. The images are of resolution 128×48 , captured from horizontal viewpoints but from widely different directions. The **PRID450s** dataset [25] consists of 450 image pairs recorded from two different static surveillance cameras. The **CAVIAR** dataset [7] consists of 1,220 images of 72 individuals from 2 cameras in a shopping mall. The number of images per person varies from 10 to 20 and image resolution also varies significantly from 141×72 to 39×17 . The **3DPeS** dataset [2] has 1,011 images of 192 individuals, with 2 to 6 images per person. The dataset is captured from 8 outdoor cameras with horizontal but significantly different viewpoints. Finally the **iLIDS** dataset [45] contains 476 images and 119 persons, with 2 to 8 images per individual. It is captured from a horizontal view point at an airport.

We compare our method against the current state-of-the-art baselines rPCCA, LMNN, SVMML, LFDA and KISSME. A brief overview of these methods is given in section 2. rPCCA, LMNN, SVMML are iterative methods whereas LFDA and KISSME are spectral methods on the second order statistics of the data. Since WARCA, rPCCA,

LMNN and LFDA are kernel methods we used both the χ^2 kernel and the linear kernel with them to benchmark the performance. Please note that the original LMNN algorithm is a linear method but we extend it to kernel space to have a thorough evaluation. We used the kernelization technique for LMNN described by Torresani *et-al.* [30]. We also used pre-conditioning to solve kernelized LMNN efficiently. Marginal Fisher discriminant analysis (MFA) is proven to give similar result as that of LFDA so we do not use them as the baseline. We also do not compare against ITML because many researchers have evaluated it before [23, 15, 18] and found out that it does not perform as well as other methods considered here.

4.2. Technical details

For the Market-1501 dataset we used the experimental protocol and features described in [44]. We used their baseline code and features, provided on the web [21]. As Market-1501 is quite large for kernel methods we do not evaluate them. We also do not evaluate the linear methods such as Linear rPCCA, LMNN and SVMML because their optimization algorithms were found to be very slow.

All other evaluations were carried out in the single-shot experiment setting [11] and our experimental settings are very similar to the one adopted by Xiong *et al.* [38]. Except for Market-1501, we randomly divided all the other datasets into two subsets such that there are p individuals in the test set. We created 10 such random splits. In each partition one image of each person was randomly selected as a probe image, and the rest of the images were used as gallery images and this was repeated 20 times. The position of the correct match was processed to generate the CMC curve. P was chosen to be 730, 119, 480, 316, 225, 36, 95 and 60 for CUHK03, OpeReid, CUHK01, VIPeR, PRID450s, CAVIAR, 3DPeS and iLIDS respectively.

We used the same set of features for all the datasets except for the Market-1501 and all the features are essentially histogram based. First all the datasets were re-scaled to 128×48 resolution and then 16 bin color histograms on RGB, YUV, and HSV channels, as well as texture histogram based on Local Binary Patterns (LBP) were extracted on 6 non-overlapping horizontal patches. All the histograms are normalized per patch to have unit L_1 norm and concatenated into a single vector of dimension 2,580 [23, 38].

The source codes for LFDA, KISSME and SVMML are available from their respective authors website, and we used those to reproduce the baseline results [38]. The code for PCCA is not released publicly. A version from Xiong *et al.* [38] is available publicly but the memory footprint of that implementation is very high making it impossible to use with large datasets (e.g. it requires 17GB of RAM to run on the CAVIAR dataset). Therefore to reproduce the results in [38] we wrote our own implementation, which uses 30

Dataset	WARCA- χ^2	WARCA-L	rPCCA- χ^2	rPCCA-L	LMNN- χ^2	LMNN-L	SVMML	LFDA- χ^2	LFDA-L	KISSME
Market-1501	—	0.45±0.00	—	—	—	—	—	—	0.34±0.00	0.43±0.00
CUHK03	0.55±0.00	0.36±0.01	0.50±0.00	0.35±0.01	0.36±0.01	0.33±0.00	0.21±0.01	0.48±0.01	0.33±0.01	0.33±0.00
CUHK01	0.58±0.01	0.37±0.01	0.49±0.01	0.35±0.01	0.30±0.01	0.31±0.01	0.28±0.01	0.55±0.01	0.34±0.01	0.36±0.01
OpeReid	0.58±0.02	0.44±0.01	0.53±0.02	0.44±0.01	0.32±0.01	0.34±0.01	0.31±0.02	0.54±0.02	0.43±0.01	0.42±0.01
VIPeR	0.33±0.01	0.21±0.01	0.22±0.02	0.16±0.01	0.18±0.01	0.15±0.01	0.23±0.02	0.31±0.02	0.20±0.02	0.21±0.01
PRID450s	0.25±0.02	0.10±0.01	0.16±0.01	0.08±0.01	0.14±0.02	0.08±0.01	0.13±0.02	0.24±0.01	0.03±0.01	0.15±0.02
CAVIAR	0.43±0.02	0.39±0.02	0.38±0.02	0.27±0.02	0.30±0.02	0.32±0.01	0.27±0.02	0.41±0.02	0.38±0.02	0.32±0.02
3DPeS	0.52±0.02	0.44±0.02	0.46±0.02	0.33±0.02	0.34±0.02	0.37±0.03	0.30±0.02	0.51±0.01	0.43±0.03	0.38±0.02
iLIDS	0.37±0.02	0.32±0.03	0.27±0.03	0.23±0.03	0.18±0.02	0.21±0.02	0.21±0.03	0.36±0.02	0.33±0.03	0.28±0.04

(a) Rank 1 accuracy.

Dataset	WARCA- χ^2	WARCA-L	rPCCA- χ^2	rPCCA-L	LMNN- χ^2	LMNN-L	SVMML	LFDA- χ^2	LFDA-L	KISSME
Market-1501	—	0.68±0.00	—	—	—	—	—	—	0.52±0.00	0.62±0.00
CUHK03	0.76±0.01	0.55±0.01	0.74±0.01	0.56±0.01	0.45±0.01	0.43±0.01	0.45±0.01	0.68±0.01	0.45±0.01	0.47±0.00
CUHK01	0.80±0.01	0.59±0.01	0.74±0.01	0.57±0.02	0.43±0.01	0.45±0.01	0.54±0.02	0.76±0.01	0.49±0.01	0.54±0.01
OpeReid	0.80±0.02	0.67±0.01	0.78±0.02	0.68±0.01	0.43±0.01	0.47±0.01	0.60±0.01	0.75±0.02	0.60±0.01	0.62±0.02
VIPeR	0.66±0.02	0.50±0.02	0.54±0.02	0.43±0.02	0.48±0.02	0.40±0.02	0.55±0.02	0.65±0.02	0.45±0.02	0.48±0.02
PRID450s	0.56±0.02	0.32±0.03	0.44±0.02	0.27±0.02	0.38±0.02	0.28±0.03	0.38±0.02	0.55±0.02	0.13±0.01	0.37±0.02
CAVIAR	0.74±0.03	0.68±0.02	0.71±0.02	0.57±0.02	0.54±0.03	0.56±0.02	0.62±0.04	0.69±0.03	0.62±0.03	0.61±0.03
3DPeS	0.76±0.03	0.68±0.02	0.74±0.02	0.58±0.02	0.59±0.03	0.61±0.03	0.60±0.03	0.75±0.02	0.66±0.02	0.60±0.02
iLIDS	0.66±0.02	0.59±0.03	0.57±0.03	0.52±0.04	0.44±0.03	0.48±0.03	0.51±0.04	0.65±0.03	0.60±0.03	0.54±0.04

(b) Rank 5 accuracy.

Dataset	WARCA- χ^2	WARCA-L	rPCCA- χ^2	rPCCA-L	LMNN- χ^2	LMNN-L	SVMML	LFDA- χ^2	LFDA-L	KISSME
Market-1501	—	0.75±0.00	—	—	—	—	—	—	0.60±0.00	0.70±0.00
CUHK03	0.83±0.00	0.65±0.01	0.81±0.00	0.67±0.01	0.49±0.01	0.48±0.01	0.59±0.01	0.76±0.00	0.53±0.01	0.56±0.01
CUHK01	0.85±0.01	0.69±0.01	0.81±0.01	0.68±0.01	0.53±0.02	0.55±0.01	0.66±0.01	0.82±0.01	0.58±0.01	0.63±0.01
OpeReid	0.86±0.01	0.77±0.01	0.85±0.01	0.77±0.01	0.50±0.01	0.55±0.01	0.74±0.01	0.83±0.01	0.69±0.02	0.71±0.01
VIPeR	0.79±0.01	0.67±0.01	0.71±0.02	0.62±0.01	0.67±0.02	0.59±0.02	0.71±0.02	0.79±0.01	0.63±0.01	0.65±0.01
PRID450s	0.72±0.01	0.50±0.02	0.63±0.02	0.46±0.02	0.58±0.02	0.47±0.02	0.60±0.01	0.72±0.02	0.28±0.01	0.54±0.02
CAVIAR	0.86±0.01	0.83±0.01	0.84±0.01	0.77±0.01	0.69±0.03	0.72±0.02	0.79±0.02	0.82±0.02	0.77±0.02	0.79±0.02
3DPeS	0.84±0.02	0.78±0.02	0.83±0.01	0.72±0.02	0.71±0.01	0.73±0.02	0.73±0.02	0.83±0.01	0.76±0.01	0.72±0.01
iLIDS	0.79±0.02	0.73±0.02	0.74±0.02	0.70±0.02	0.65±0.03	0.67±0.03	0.70±0.02	0.79±0.01	0.74±0.02	0.70±0.03

(c) AUC score.

Table 2: Table showing the rank 1, rank 5 and AUC performance measure of our method WARCA against other state-of-the-art methods. Bold fields indicate best performing methods. The dashes indicate computation that could not be run in a realistic setting on Market-1501.

times less memory and can scale to much larger datasets. We also ran sanity checks to make sure that it behaves the same as that of the baseline code.

All the implementations were done in Matlab with mex functions for the acceleration of the critical components. For WARCA and rPCCA we implemented the entire algorithms in C++ with BLAS and OpenMP to have a fair comparison on their running times.

4.3. Results

In order to fairly evaluate the algorithms, we set the dimensionality of the projected space to be same for WARCA, LMNN, rPCCA and LFDA. For the Market-1501 dataset the dimensionality used is 200 and for all the other datasets it is 40. We choose the regularization parameter and the learning rate through cross-validation across the data splits using grid search in $(\lambda, \eta) \in \{10^{-8}, \dots, 1\} \times \{10^{-3}, \dots, 1\}$. Margin γ is fixed to 1. Since the size of the parameter matrix scales in $O(D^2)$ for SVMML and KISSME we first reduced the dimension of the original features using PCA keeping 95% of the original variance and then applied these algorithms. In our tables and

figures WARCA- χ^2 , WARCA-L, rPCCA- χ^2 , rPCCA-L, LMNN- χ^2 , LMNN-L, LFDA- χ^2 and LFDA-L denote WARCA with χ^2 kernel, WARCA with linear kernel, rPCCA with χ^2 kernel, rPCCA with linear kernel, LMNN with χ^2 kernel, LMNN with linear kernel and LFDA with χ^2 kernel, LFDA with linear kernel respectively.

For all experiments with WARCA we used harmonic weighting for the rank weighting function 8. That is weighting of the form $\mathcal{H}(M) = \sum_{m=1}^M \frac{1}{m}$. We also tried uniform weighting which gave poor results compared to the harmonic weighting for a given computational budget. For all the datasets we used a mini-batch size of 512 in the SGD algorithm and we ran the SGD for 2000 iterations (A parameter update using the mini-batch is considered as 1 iteration).

Tables 2a and 2b summarize respectively the rank-1 and rank-5 performance of all the methods, and table 2c summarizes the Area Under the Curve (AUC) performance score. Figure 2 reports the CMC curves comparing WARCA against the baselines on all the nine datasets. The circle and the star markers denote linear and kernel methods respectively.

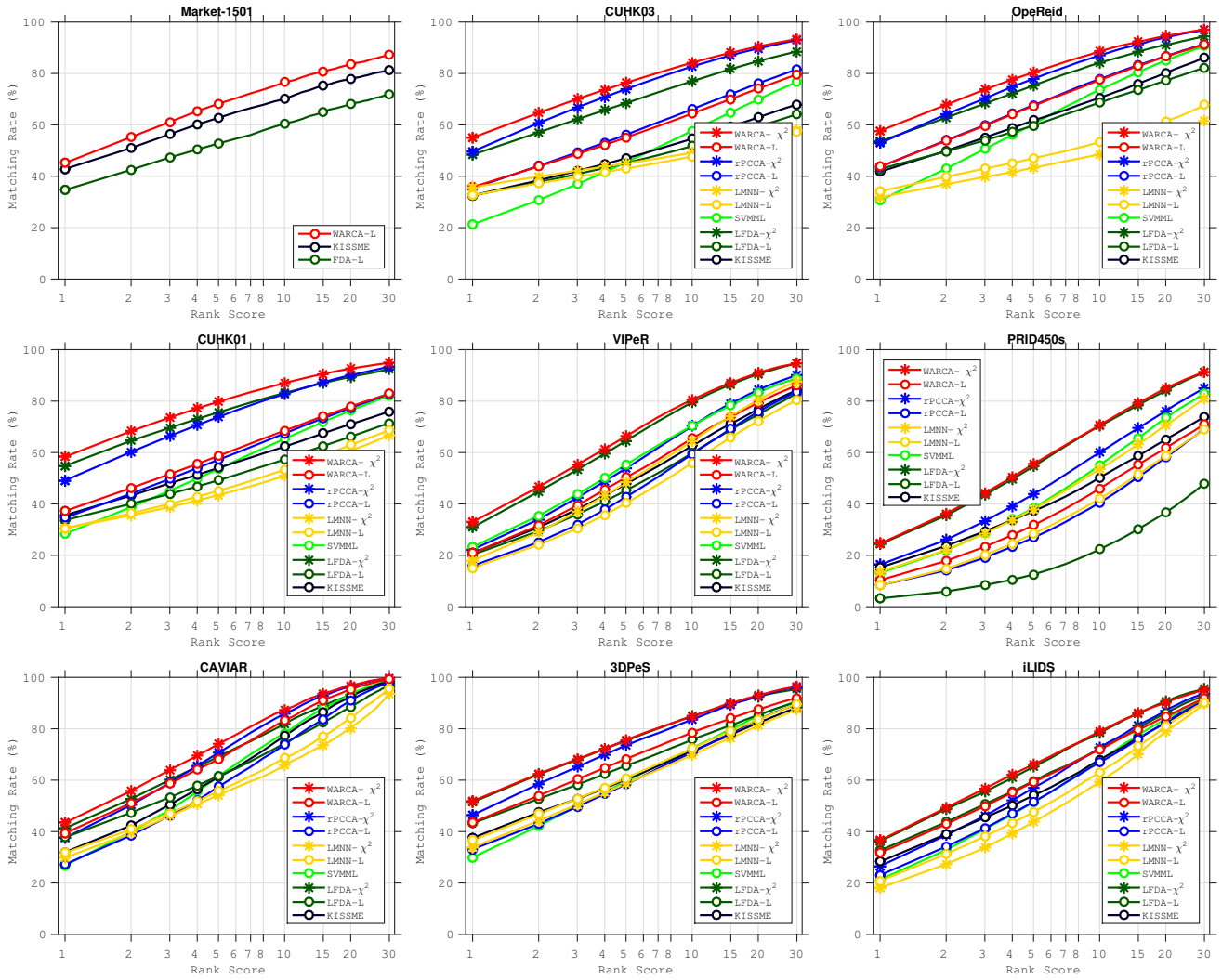


Figure 2: CMC curves comparing WARCA against state-of-the-art methods on nine re-identification datasets

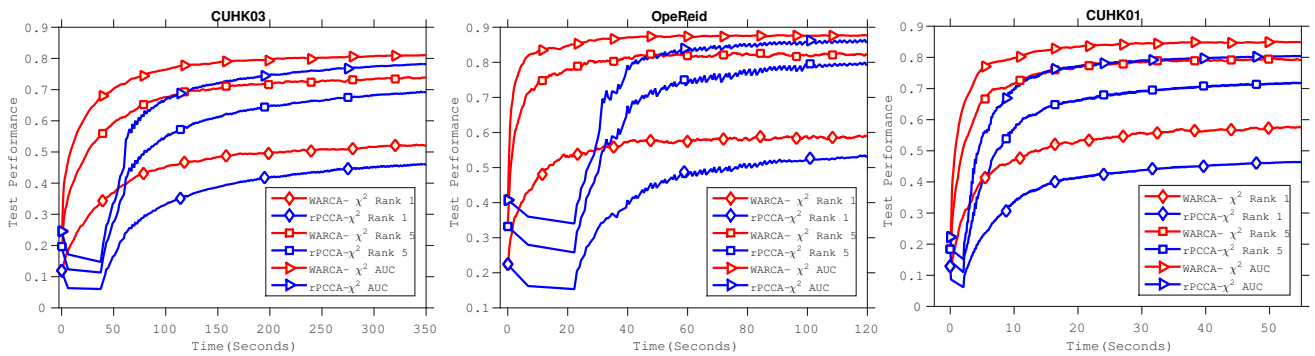


Figure 3: WARCA performs significantly better than the current state-of-the-art rPCCA on large datasets for a given training time budget.

WARCA improves over all other methods on all the datasets. On 3DPeS, PRID450s and iLIDS

LFDA come very close to the performance of WARCA. The reason for this is that these datasets are too small and consequently

Dataset	WARCA- χ^2	WARCA-L	FRML	MLPOLY	IDEEP
CUHK03-100TID	0.74±0.01	0.62±0.02	0.54±0.02	—	0.5474
CUHK01-100TID	0.77±0.02	0.60±0.03	0.54±0.02	—	0.6500
CUHK01-486TID	0.58±0.01	0.39±0.01	0.34±0.00	—	0.4753
VIPeR-CameralID	0.37±0.01	0.22±0.01	0.18±0.01	0.3680	0.3481
CAVIAR	0.43±0.02	0.39±0.02	0.34±0.02	0.4010	—

Table 3: Rank 1 accuracy. TID indicates the number of test identities.

simple methods such as LFDA which exploits strong prior assumptions on the data distribution work nearly as well as WARCA.

Figure 3 illustrates how the test set performance of WARCA and rPCCA increase as a function of training time on 3 datasets. Please note that we do not include spectral methods in this plot because its solutions are found analytically. Linear spectral methods are very fast for low dimensional problems but the training time scales quadratically in the data dimension. In case of kernel spectral methods the training time scales quadratically in the number of data points. We also do not include iterative methods, LMNN and SVMML because they proved to be very slow and not giving good performance.

4.4. Additional results

We are also including additional comparisons against recent algorithms for re-identification such as MLPOLY [6], IDEEP [1]. The reason for not including these results in main results is because the code for these methods are not available and the features are different which makes a fair comparison difficult. Our goal is to experimentally evaluate that, given a set of features which is the best off-the-shelf metric learning algorithm of re-identification. To have a fair comparisons we did exactly the same train-test split as the baselines. For CUHK03 train identities = 1160, test identities(TID) = 100. For CUHK01 we conducted 2 sets of experiments like in IDEEP ie with 100 test id and 486 test id. Please not that in the original experiments we were no t using camera id information for VIPeR during testing which makes the problem difficult. The new results are with camera-id information exactly like in the baselines to have a close comparison. The results are summarized in the table 3. We clearly outperform all the baselines by a large margin and our method is very simple, fast and very easy to implement.

4.5. Comparisons to FRML [20]

The code for FRML [20] is available, but the published results are for retrieval. We got consistent results on the provided test, but results, even with tuning of meta-parameters on the test set are abysmal for re-identification. This may be explained in part by their implementation. We re-implemented the method and run additional experiments and could not get better than ours 3.

Regarding the similarity between the methods, the loss function is the same as our linear method, but both the optimization scheme and the regularizer differ. FRML is a linear method which uses L2 or LMNN regularizer. Moreover it has an expensive projection step in the SGD and for that it has to keep a record on all the points seen in the mini-batch which results in high memory foot print. Their rationale for the projection step is to accelerate the SGD because directly optimizing low rank W may result in W not invariant to orthonormal transformation ie $W^T W \neq I$ and result in non-isolated minimizers. We approximately get rid of this issue very efficiently by using our approximate orthonormal regularizer. Thus our approach is far more efficient computationally.

We did not compare against other ranking based metric learning methods such as LORETA [27], OASIS [5] and MLR [22] because of all of them are linear methods. Infact we derived a kernelized OASIS but the results were not as good as ours or rPCCA.

5. Conclusion and Future work

We have proposed a simple and scalable approach to metric learning by optimizing a weighted sum of the precision at different ranks, which can be used for any weighting of the precision-at- k metrics. Experimental results show that it performs well on standard person re-identification datasets.

Our future works will target two main axes. The first is to asses WARCA on even larger datasets of 1 or 2 order of magnitude larger. The second is to investigate other embeddings in WARCA instead of Mahalanobis distance. Since WARCA is very general, it can be straightforwardly used with other embeddings such as convolutional neural network or random forest.

References

- [1] E. Ahmed, M. Jones, and T. K. Marks. An improved deep learning architecture for person re-identification. In *Proceedings of the IEEE Conference on Computer Vision and Pattern Recognition*, pages 3908–3916, 2015. 9
- [2] D. Baltieri, R. Vezzani, and R. Cucchiara. 3dpes: 3d people dataset for surveillance and forensics. In *Proceedings of the 2011 joint ACM workshop on Human gesture and behavior understanding*, pages 59–64. ACM, 2011. 2, 6
- [3] S. Boyd and L. Vandenberghe. *Convex Optimization*. Cambridge University Press, 2004. 2
- [4] O. Chapelle. Training a support vector machine in the primal. *Neural Computation*, 19(5):1155–1178, 2007. 1, 6
- [5] G. Chechik, V. Sharma, U. Shalit, and S. Bengio. Large scale online learning of image similarity through ranking. *The Journal of Machine Learning Research*, 11:1109–1135, 2010. 9
- [6] D. Chen, Z. Yuan, G. Hua, N. Zheng, and J. Wang. Similarity learning on an explicit polynomial kernel feature map for

- person re-identification. In *Proceedings of the IEEE Conference on Computer Vision and Pattern Recognition*, pages 1565–1573, 2015. 9
- [7] D. S. Cheng, M. Cristani, M. Stoppa, L. Bazzani, and V. Murino. Custom pictorial structures for re-identification. In *British Machine Vision Conference (BMVC)*, 2011. 1, 2, 6
- [8] J. V. Davis, B. Kulis, P. Jain, S. Sra, and I. S. Dhillon. Information-theoretic metric learning. In *Proceedings of the 24th annual International Conference on Machine Learning (ICML-07)*, pages 209–216. ACM, 2007. 2
- [9] M. Farenzena, L. Bazzani, A. Perina, V. Murino, and M. Cristani. Person re-identification by symmetry-driven accumulation of local features. In *Computer Vision and Pattern Recognition (CVPR), 2010 IEEE Conference on*, pages 2360–2367. IEEE, 2010. 1
- [10] P. Felzenszwalb, D. McAllester, and D. Ramanan. A discriminatively trained, multiscale, deformable part model. In *Computer Vision and Pattern Recognition, 2008. CVPR 2008. IEEE Conference on*, pages 1–8. IEEE, 2008. 6
- [11] S. Gong, M. Cristani, S. Yan, and Loy, editors. *Person Re-Identification*. Advances in Computer Vision and Pattern Recognition. Springer, 2014. 1, 6
- [12] D. Gray and H. Tao. Viewpoint invariant pedestrian recognition with an ensemble of localized features. In *Computer Vision—ECCV 2008*, pages 262–275. Springer, 2008. 2, 6
- [13] P. Jain, B. Kulis, J. V. Davis, and I. S. Dhillon. Metric and kernel learning using a linear transformation. *The Journal of Machine Learning Research*, 13(1):519–547, 2012. 2
- [14] M. Journée, F. Bach, P.-A. Absil, and R. Sepulchre. Low-rank optimization on the cone of positive semidefinite matrices. *SIAM Journal on Optimization*, 20(5):2327–2351, 2010. 2
- [15] M. Köstinger, M. Hirzer, P. Wohlhart, P. M. Roth, and H. Bischof. Large scale metric learning from equivalence constraints. In *Computer Vision and Pattern Recognition (CVPR), 2012 IEEE Conference on*, pages 2288–2295. IEEE, 2012. 1, 2, 6
- [16] W. Li, R. Zhao, and X. Wang. Human reidentification with transferred metric learning. In *ACCV (I)*, pages 31–44, 2012. 2, 6
- [17] W. Li, R. Zhao, T. Xiao, and X. Wang. Deepreid: Deep filter pairing neural network for person re-identification. In *Computer Vision and Pattern Recognition (CVPR), 2014 IEEE Conference on*, pages 152–159. IEEE, 2014. 2, 6
- [18] Z. Li, S. Chang, F. Liang, T. S. Huang, L. Cao, and J. R. Smith. Learning locally-adaptive decision functions for person verification. In *Computer Vision and Pattern Recognition (CVPR), 2013 IEEE Conference on*, pages 3610–3617. IEEE, 2013. 1, 2, 6
- [19] S. Liao, Z. Mo, Y. Hu, and S. Z. Li. Open-set person re-identification. *arXiv preprint arXiv:1408.0872*, 2014. 2, 6
- [20] D. Lim and G. Lanckriet. Efficient learning of mahalanobis metrics for ranking. In *Proceedings of the 31st International Conference on Machine Learning (ICML-14)*, pages 1980–1988, 2014. 1, 3, 4, 9
- [21] Market-1501 data-set. http://www.liangzheng.org/Project/project_reid.html. 6
- [22] B. McFee and G. R. Lanckriet. Metric learning to rank. In *Proceedings of the 27th annual International Conference on Machine Learning (ICML-10)*, pages 775–782, 2010. 2, 9
- [23] A. Mignon and F. Jurie. Pcca: A new approach for distance learning from sparse pairwise constraints. In *Computer Vision and Pattern Recognition (CVPR), 2012 IEEE Conference on*, pages 2666–2672. IEEE, 2012. 1, 2, 5, 6
- [24] S. Paisitkriangkrai, C. Shen, and A. van den Hengel. Learning to rank in person re-identification with metric ensembles. In *IEEE Conference on Computer Vision and Pattern Recognition (CVPR)*, 2015. 2
- [25] P. M. Roth, M. Hirzer, M. Köstinger, C. Beleznaï, and H. Bischof. Mahalanobis distance learning for person re-identification. In *Person Re-Identification*, pages 247–267. Springer, 2014. 2, 6
- [26] S. Shalev-Shwartz and S. Ben-David. *Understanding Machine Learning: From Theory to Algorithms*. Cambridge University Press, 2014. 4
- [27] U. Shalit, D. Weinshall, and G. Chechik. Online learning in the embedded manifold of low-rank matrices. *The Journal of Machine Learning Research*, 13(1):429–458, 2012. 9
- [28] M. Sugiyama. Local fisher discriminant analysis for supervised dimensionality reduction. In *Proceedings of the 23rd annual International Conference on Machine Learning (ICML-06)*, pages 905–912. ACM, 2006. 2
- [29] I. Sutskever. *Training recurrent neural networks*. PhD thesis, University of Toronto, 2013. 4
- [30] L. Torresani and K.-c. Lee. Large margin component analysis. In *Advances in neural information processing systems*, pages 1385–1392, 2006. 6
- [31] I. Tsochantaridis, T. Hofmann, T. Joachims, and Y. Altun. Support vector machine learning for interdependent and structured output spaces. In *Proceedings of the 21st annual International Conference on Machine Learning (ICML-04)*, page 104. ACM, 2004. 2
- [32] N. Usunier, D. Buffoni, and P. Gallinari. Ranking with ordered weighted pairwise classification. In *Proceedings of the 26th annual International Conference on Machine Learning (ICML-09)*, pages 1057–1064. ACM, 2009. 4
- [33] A. Vedaldi and A. Zisserman. Efficient additive kernels via explicit feature maps. *Pattern Analysis and Machine Intelligence, IEEE Transactions on*, 34(3):480–492, 2012. 5
- [34] K. Q. Weinberger and L. K. Saul. Distance metric learning for large margin nearest neighbor classification. *The Journal of Machine Learning Research*, 10:207–244, 2009. 1, 2
- [35] J. Weston, S. Bengio, and N. Usunier. WSABIE: Scaling up to large vocabulary image annotation. In *IJCAI*, volume 11, pages 2764–2770, 2011. 1, 3, 4
- [36] Y. Wu, M. Mukunoki, T. Funatomi, M. Minoh, and S. Lao. Optimizing mean reciprocal rank for person re-identification. In *Advanced Video and Signal-Based Surveillance (AVSS), 2011 8th IEEE International Conference on*, pages 408–413. IEEE, 2011. 2
- [37] E. P. Xing, M. I. Jordan, S. Russell, and A. Y. Ng. Distance metric learning with application to clustering with side-information. In *Advances in neural information processing systems*, pages 505–512, 2002. 2

- [38] F. Xiong, M. Gou, O. Camps, and M. Sznajder. Person re-identification using kernel-based metric learning methods. In *Computer Vision–ECCV 2014*, pages 1–16. Springer, 2014. [1](#), [2](#), [6](#)
- [39] S. Yan, D. Xu, B. Zhang, H.-J. Zhang, Q. Yang, and S. Lin. Graph embedding and extensions: a general framework for dimensionality reduction. *Pattern Analysis and Machine Intelligence, IEEE Transactions on*, 29(1):40–51, 2007. [2](#)
- [40] L. Yang and R. Jin. Distance metric learning: A comprehensive survey. *Michigan State University*, 2, 2006. [2](#)
- [41] J. Zhang, M. Marszałek, S. Lazebnik, and C. Schmid. Local features and kernels for classification of texture and object categories: A comprehensive study. *International journal of computer vision*, 73(2):213–238, 2007. [5](#)
- [42] R. Zhao, W. Ouyang, and X. Wang. Unsupervised saliency learning for person re-identification. In *Computer Vision and Pattern Recognition (CVPR), 2013 IEEE Conference on*, pages 3586–3593. IEEE, 2013. [1](#)
- [43] R. Zhao, W. Ouyang, and X. Wang. Learning mid-level filters for person re-identification. In *Computer Vision and Pattern Recognition (CVPR), 2014 IEEE Conference on*, pages 144–151. IEEE, 2014. [1](#)
- [44] L. Zheng, L. Shen, L. Tian, S. Wang, J. Wang, J. Bu, and Q. Tian. Scalable person re-identification: A benchmark. *Computer Vision, IEEE International Conference on*, 2015. [2](#), [6](#)
- [45] W.-S. Zheng, S. Gong, and T. Xiang. Associating groups of people. In *British Machine Vision Conference (BMVC)*, volume 2, page 6, 2009. [2](#), [6](#)